AFRL-RX-WP-TR-2023-0057

ASSESSMENT OF TEST METHODS FOR MEASURING HIGH TEMPERATURE TENSILE PROPERTIES OF SUBSCALE SPECIMEN GEOMETRIES FOR ADDITIVELY MANUFACTURED METALLIC MATERIALS

Thomas Gallmeyer
AFRL/RXNMB

15 MAY 2023
Interim Report

AIR FORCE RESEARCH LABORATORY
MATERIALS AND MANUFACTURING DIRECTORATE
WRIGHT-PATTERSON AIR FORCE BASE, OH 45433-7750
AIR FORCE MATERIEL COMMAND
UNITED STATES AIR FORCE

NOTICE AND SIGNATURE PAGE

Using Government drawings, specifications, or other data included in this document for any purpose other than Government procurement does not in any way obligate the U.S. Government. The fact that the Government formulated or supplied the drawings, specifications, or other data does not license the holder or any other person or corporation; or convey any rights or permission to manufacture, use, or sell any patented invention that may relate to them.

This report is cleared for public release by Air Force Research Laboratory Public Affairs Office (AFRL/PA) and is available to the general public, including foreign nationals. This report is available to the general public, including foreign nationals. Copies may be obtained from the Defense Technical Information Center (DTIC) (http://www.dtic.mil).

AFRL-RX-WP-TR-2023-0057 HAS BEEN REVIEWED AND IS APPROVED FOR PUBLICATION IN ACCORDANCE WITH ASSIGNED DISTRIBUTION STATEMENT.

GALLMEYER.THOMAS.GERALD.1594731618
Digitally signed by GALLMEYER.THOMAS.GERALD.1594731618
Date: 2023.05.31 16:00:27 -04'00'

THOMAS G. GALLMEYER
Research Materials Engineer
Materials Behavior and Response Section
Metals Branch
Composite, Ceramic, Metallic, and
Materials Performance Division
Materials and Manufacturing Directorate

LEE.DAVID.S.1075806597
Digitally signed by LEE.DAVID.S.1075806597
Date: 2023.05.31 16:38:09 -04'00'

DAVID S. LEE
Branch Chief
Metals Branch
Composite, Ceramic, Metallic, and
Materials Performance Division
Materials and Manufacturing Directorate

This report is published in the interest of scientific and technical information exchange, and its publication does not constitute the Government's approval or disapproval of its ideas or findings.

REPORT DOCUMENTATION PAGE

PLEASE DO NOT RETURN YOUR FORM TO THE ABOVE ORGANIZATION.

1. REPORT DATE	2. REPORT TYPE	3. DATES COVERED	
		START DATE	END DATE
15 May 2023	Interim	27 February 2020	05 May 2023

4. TITLE AND SUBTITLE

ASSESSMENT OF TEST METHODS FOR MEASURING HIGH TEMPERATURE TENSILE PROPERTIES OF SUBSCALE SPECIMEN GEOMETRIES FOR ADDITIVELY MANUFACTURED METALLIC MATERIALS

5a. CONTRACT NUMBER	5b. GRANT NUMBER	5c. PROGRAM ELEMENT NUMBER
In-House		
5d. PROJECT NUMBER	**5e. TASK NUMBER**	**5f. WORK UNIT NUMBER**
		X20M

6. AUTHOR(S)

Thomas Gallmeyer

7. PERFORMING ORGANIZATION NAME(S) AND ADDRESS(ES)

AFRL/RXNMB
Materials and Manufacturing Directorate
2230 Tenth Street, Suite 1
Wright-Patterson AFB, OH 45433-7750

8. PERFORMING ORGANIZATION REPORT NUMBER

AFRL-RX-WP-TR-2023-0057

9. SPONSORING/MONITORING AGENCY NAME(S) AND ADDRESS(ES)	10. SPONSOR/MONITOR'S ACRONYM(S)	11. SPONSOR/MONITOR'S REPORT NUMBER(S)
Air Force Research Laboratory Materials and Manufacturing Directorate Wright-Patterson Air Force Base, OH 45433-7750 Air Force Materiel Command United States Air Force	AFRL/RXNMB	AFRL-RX-WP-TR-2023-0057

12. DISTRIBUTION/AVAILABILITY STATEMENT

DISTRIBUTION STATEMENT A. Approved for public release: distribution unlimited.

13. SUPPLEMENTARY NOTES

PA Clearance Number: (Number) AFRL-2023-2626, 30 May 2023.

14. ABSTRACT

An overview of the state-of-the-art for subscale high temperature tensile testing of metallic materials is reported. Presented in this report are current subscale specimen geometries and design considerations, test setup and instrumentations, and considerations for the assessment of additively manufactured metallic materials.

15. SUBJECT TERMS

subscale specimen geometry, tensile testing, high temperature, additive manufacturing

16. SECURITY CLASSIFICATION OF:			17. LIMITATION OF ABSTRACT	18. NUMBER OF PAGES
a. REPORT	b. ABSTRACT	C. THIS PAGE		
Unclassified	Unclassified	Unclassified	SAR	38

19a. NAME OF RESPONSIBLE PERSON	19b. PHONE NUMBER *(Include area code)*
Thomas Gallmeyer	(937) 255-0485

PREVIOUS EDITION IS OBSOLETE

STANDARD FORM 298 (REV. 5/2020)

Prescribed by ANSI Std. Z39.18

TABLE OF CONTENTS

Section **Page**

LIST OF FIGURES

LIST OF TABLES

1.0 EXECUTIVE SUMMARY

As additive manufacturing matures, its implementation is desired to support the production of low-quantity, cost-effective and/or difficult-to-manufacture components for high temperature applications. Yet, challenges exist for how to qualify additively manufactured components, especially when location-specific performance may vary. Small feature sizes may limit the material volume available for performance characterization; therefore, subscale test methods are ideally suited. This report provides a short review of current test methods for high temperature tensile testing of subscale specimen geometries to identify technological gaps and limitations, to offer recommendations for future research directions to improve test methods, and to discuss testing considerations specific to the evaluation of additively manufactured metallic materials. The report concludes that the guiding principles for high temperature tensile testing of standard specimens are generally the same for subscale specimens. Specimen geometry design most often directly scales down from standardized test coupons with minimum size limits bounded by material-specific properties and microstructures as to ensure a comparable bulk response. Overwhelmingly, it is found that subscale tensile testing utilizes flat specimen geometries. It is also concluded that high temperature subscale tensile testing would greatly benefit from further development of current non-contact measurement methods for temperature and strain.

Considerations addressed for the evaluation of additively manufactured metallic materials largely emanate from the effects as-built surface finish have on mechanical performance. High-throughput testing may be necessary for a probabilistic approach to predicting minimum performance limits that captures the inherent variability of additive manufacturing processes.

It is recommended that non-destructive inspection methodologies be developed and standardized for the accurate measurement of the true load-bearing area of thin-walled geometries with retained as-built surfaces as it is identified as a significant source of measurement error. Additionally, it is recommended that a select number of subscale specimen geometries be chosen to establish guidelines for design. Efforts are currently underway to establish these guidelines by ASTM Subcommittees E28.04.01 and F42.01, but the efforts only are targeting room temperature evaluation in scope.

2.0 INTRODUCTION

With the rise of additive manufacturing (AM) for metallic materials, concerted efforts are underway to integrate the technology into present and future aerospace systems to enhance performance capability, reduce cost, and minimize production lead-times. One advantage of AM components is the generation of complex and thin-walled geometries for location-specific performance otherwise unachievable through conventional manufacturing means. Yet, as a new manufacturing process, AM leads to unique microstructures that must be properly assessed for material properties and performance. At times, regions of interest at the component level will require subscale specimen excision and evaluation for proper characterization as witness coupons may not fully capture location-specific performance. Other industries, e.g., nuclear power, have adopted non-standardized testing with the goal of test specimen miniaturization so to characterize material response using minimal material volume without the sacrifice of accurately capturing bulk material properties. Material scarcity, costs, and handling hazards all motivate the need for developing such a testing capability.

As such, the aim of this report is to review the standards and practices around high temperature tensile testing with particular focus on the current state-of-the-art for subscale test methods. First, Section 3.0 will present standard and non-standard approaches to the design of subscale specimen geometries, in addition to providing an overview of existing test equipment, instrumentation, and setup. Next, Section 4.0 discusses the identified technological gaps in test methods, size-dependent responses of subscale specimens, and considerations for the evaluation of AM-produced metallic material. In conclusion, Sections 5.0 and 6.0, respectively, will summarily state insights drawn about the effectiveness of the presented methods, as well as provide recommendations for future work to advance the field.

Lastly, the scope of this report will exclude high temperature testing using electron microscopy equipment. The reader is encouraged to review the listed resources for information on the topic area [1]–[6].

3.0 CURRENT METHODOLOGIES, EQUIPMENT, AND INSTRUMENTATION

Two of the principal standards recognized for elevated temperature tensile testing of metallic materials are ASTM E21 and ISO 6892-2. Notably, these standards heavily pull from their room temperature equivalents – ASTM E8 and ISO 6892-1 – to specify acceptable specimen geometries and general test setup. However, none of the standards directly addresses how to approach the intricacies specific to subscale specimen testing. The most frequently reported approaches from literature to specimen design, equipment, instrumentation, and their setups are presented in this section.

3.1 Tensile Specimen Geometries

There are current efforts within ASTM Subcommittee E28.04.01 (Task Group on Small Specimens in E8/E8M) to publish an annex providing guidelines to uniaxial tensile testing of subscale geometries. Yet, the annex has limited scope to room temperature evaluation only. Additional efforts are underway through ASTM Subcommittee F42.01 (New Test Method for Additive Manufacturing – Test Artifacts – Miniature Tension Testing of Metallic Materials), which seeks to develop a miniature rectangular cross-section tension specimen with a gauge length of 10-15 mm. However, the title and scope of the effort presently is in draft form. A summary of standard and non-standard (i.e., subscale) specimen geometries and test methods will now be given.

3.1.1 Standard

ASTM E8 and ISO 6892-1 provide guidance on acceptable standard tensile specimen geometries. A generalized specimen layout is presented in Figure 1 while a summary for the parametric design of round and flat specimen geometries shown in Table 1. The ratios have been established to bound the design parameters to ensure proportional response, i.e., interlaboratory comparability. Often, standard geometries serve as the basis for subscale specimen design. ASTM E8 specifically outlines a subsize geometry for rectangular tension test specimens. The subsize specimen has a gauge length of 25.0 mm, width of 6.0 mm, and variable thickness not to exceed the width dimension. Yet, despite explicitly defining a subsize geometry, the scale of its standardized form remains large in the context of subscale testing. Hence, efforts have been undertaken to retain high fidelity assessment while minimizing material volumes.

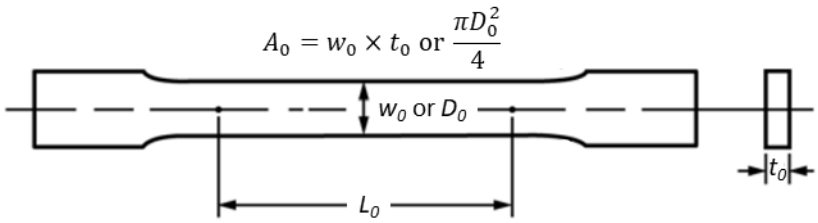

Figure 1. Generalized Specimen Geometry from ASTM E8 and ISO 6892-1.

Table 1. Lower Limits of Tensile Specimen Design Outlined in ASTM E8 and ISO 6892-1. Adapted from [7].

Standard organization		ASTM E8	ISO 6892-1
Round specimen	Aspect ratio	$\frac{L_0}{D_0} = 4$	$\frac{L_0}{D_0} = 5$ or 10
	Lower limit of specimen size	$D_0 = 2.5$ $L_0 = 10$	$D_0 = 5$ $L_0 = 25$
	Aspect ratio	$\frac{L_0}{\sqrt{A_0}} = 4.5$	$\frac{L_0}{\sqrt{A_0}} = 5.65$ or 11.3
	Lower limit of proportional specimen size	NA	NA
Flat specimen			
	Lower limit of non-proportional specimen size	$t_0 \leq 6$ $L_0 = 25$ $w_0 = 6$	$t_0 \geq 3$ $L_0 = 80, w_0 = 20$ $0.1 < t_0 < 3$ $L_0 = 50, w_0 = 12.5$

Note — L_0: original gauge length; w_0: original width; t_0: original thickness; A_0: original area of cross section; D_0: original diameter (mm).

3.1.2 Non-standard

Presently, subscale specimen design is derived generally from standardized specimen geometries, either through simple downscaling or downscaling with further dimensional modification. Zheng et al. [7] recently reviewed the standards and practices of miniaturized tensile testing at room temperature, with a focus on design approach. The authors' survey of literature found consensus on guidelines for subscale specimen design, which are summarized below:

1. Subscale specimen design should seek to adequately represent the bulk material response from standard specimen sizes. Along the same lines, the design should seek to minimize data scatter inherent to subscale specimen testing.

2. Subscale specimen design should be devised such that it allows comparison to standard geometries by using aspect ratio requirements, e.g., gauge length to square root of area ($L_0/\sqrt{A_0}$), width to thickness (w_0/t_0), and thickness to average grain size (t_0/d). Specifically, elongation to failure in subscale specimens often deviates from its standard counterparts due to differences in deformation necking, and corrections can be achieved using inverse finite element method [8] or Bertella-Oliver formula [9].

3. Practicality of subscale specimen design should be considered. This includes assumed costs and difficulty of machining, as well as the necessary fixtures and instrumentation to measure the properties of the prospective design.

Existing subscale specimens reported in literature are summarized in Table 2. Much of the effort to miniaturize specimen sizes has been driven largely by the nuclear industry to minimize the

material volume subject to radiation exposure [6], [10]–[12]. Frequently, subscale specimen geometries stem from two basic designs: 1) dogbone [13]–[18] and 2) bowtie [10], [19]–[25]. However, several subscale geometries reported do not fit within either of these design families. For example, Partheepan et al. [26] and Džugan et al. [27] developed dumbbell shaped tensile specimens from small punch test discs. Nonetheless, all the listed subscale specimen designs have shown excellent agreement with standard size specimens. Notably, all listed studies utilized flat specimen geometries, which arises from the difficulty to reliably machine round subscale specimens.

Table 2. Existing Subscale Specimen Geometries with Rectangular Cross Sections.

Basic geometry	Designation/Author	Ref.	Dimensions (mm)		
			Gauge length	Width	Thickness
Dogbone	SS-1	[27]	20.32	1.54	0.76
	SS-2		12.7	1.13	0.25
	SS-3		7.62	2.54	0.76
	SS-J3		5.00	1.20	0.75
	Kumar et al.	[17]	3.00	1.00	0.30
		[18]	3.00	1.00	0.20
	Liu et al.	[8]	2.00	1.00	0.20
	SS-Mini	[28]	2.3	0.4	0.25
	Watring et al.	[29]	2.0	0.2	0.2
		[13]	5.08	2.54	1.00
	Džugan et al.	[30]	3.0	1.5	0.5
	Gotterbarm et al.	[31]	4.5	1.0	0.5
Bowtie	LaVan et al.	[24]	3.00	0.20	0.20
	Benzing et al.	[32]	3.00	2.54	1.27
	Heckman et al.	[33]	4	1	1
	Roach et al.	[25]	1.6	0.4	0.4
Other	Dumbbell	[26]	N/A	1.00	0.50
	Dumbbell	[27]	4.00	2.00	1.00

Note: N/A reported as specimen gauge is constructed by continuous radii between grip ends with minimum gauge width specified. All other reported geometries are tangentially blending fillets with a uniform test cross-section.

3.2 Uniaxial Test Frame Setup Overview

Universal test frames are generally either screw-driven or servohydraulic, which are both perfectly suited for uniaxial tensile testing experiments. A uniaxial test frame is comprised of several basic fixture component: loading device, a load cell, and a specimen gripping apparatus. An example of a commercially available tensile testing frame is shown in Figure 2. Load cells are available in a wide range of load limits to accommodate the sensitivity needs for a wide range of materials and specimen geometries. ASTM E74 outlines the calibration procedure for load cells and must be followed to ensure proper measurement during testing, regardless of specimen size. Further details about alignment and gripping will be provided given their overall importance to testing accuracy.

Figure 2. Overview of Universal Tensile Tester [34].

3.2.1 Alignment

Standardized testing procedures have been established to assist in test frame and specimen alignment through the quantification of bending strains and their acceptable limits during testing. Test frames may be configured with some type of universal joint that allows for concentricity and angularity adjustments for alignment. The largest contributor to bending strains originates from the test specimen-grip interface [35]. ASTM E1012, established to address adequate alignment under tensile and compressive loading, outlines the usage of strain-gaged specimens to verify test equipment alignment through a series of loading-unloading and re-gripping cycles [36]. Specific to high temperature tension testing of metallic materials, standards mandate

maximum bending strains do not exceed 10% of the axial strain [37]. Despite the existence of these standards, the issue persists where, in general, equipment is unavailable to measure maximum bending strains at elevated test temperatures [37]. As a result, often, the only viable option is to qualify the alignment at room temperature using the intended machine setup for elevating temperature testing [37].

Notably, alignment requirements are designed for standard specimen sizes [36]. Alignment procedures for test setup of subscale specimens are rarely reported in detail and seem to be generally considered a "best effort" based upon experimental expertise of the user. This is somewhat troublesome because as specimen size and gauge lengths decrease, concentric and angular misalignments become more pronounced, i.e., larger bending strains. The subscale specimens may also require higher machining tolerance for more precise alignment in the specimen-grip interface. Furthermore, subscale specimen sizes frequently make it impractical to manufacture a strain-gaged specimen for proper test frame alignment due to physical constraints. As a result, custom grips and alignment fixtures often are engineered to accommodate specifically designed subscale test specimen geometries and to ensure uniaxiality throughout testing [11], [28], [31], [38]. Self-aligning grips have also been used at room temperature [39] and elevated temperatures [16]. However, one limitation of self-aligning grips is that alignment is achieved through sufficient loading to straighten them. The requisite grip-straightening load at elevated temperatures may exceed the material strength when testing subscale specimens so careful attention must be given when performing.

Moreover, though not a standardized practice, it is possible to implement 2D or 3D digital image processing techniques (i.e., digital image correlation) to assist with specimen alignment (both standard and subscale geometries) and to evaluate pre-test strain levels at the desired temperature. However, as will be discussed in Section 3.4, this becomes exceedingly more difficult as the temperature increases.

3.2.2 Specimen Gripping

High temperature testing of subscale specimen geometries typically implements pull-rod and wedge gripping systems [8], [10], [11], [19], [21], [28], [40], [41]. For standard-sized specimens, the most used is temperature-resistant metallic alloy pull-rods (i.e., Ni-based superalloys) and threaded-end specimen grips to allow for optimal thermal uniformity and limited slippage during testing. However, this setup becomes difficult for subscale testing as 1) the practicality of machining threaded grip ends is prohibitive due to miniaturized size and 2) it requires round specimens when subscale testing almost exclusively uses flat geometries, as presented in Section 3.1.2. For subscale testing at high temperatures, pull-rods are used with bowtie specimen geometries with good success. For example, Zupan et al. [19] used tapered pull-grips to provide good mechanical and electrical contact between the miniature bowtie specimen and grips for resistance-heated high temperature tensile testing. Moreover, ceramic pull-grips have also been effective for miniature bowtie specimens for high temperature testing using radiant heating, as demonstrated by Alam et al. [41]. The machining tolerance of the subscale specimen bowtie or standard grip end may be more critical as the specimen size decreases.

Alternatively, wedge grips are used in manual or hydraulic configurations. An advantage for wedge-style gripping is the mitigation of specimen slippage during testing. Manual wedge grips

are most affordable but are particularly problematic as the rotational tightening mechanism to close the grips induces a bending moment on the specimen. Hydraulic grips are designed to eliminate this effect and apply only axial loads when gripping. The use of cold grips (e.g., water-cooled hydraulic grips) allows for the greatest mitigation of additional bending errors that can arise during heating. However, the large thermal inertia of hydraulic grips can reduce the length of the uniform heat zone in the specimen gauge. Instead, hot grips (pre-heated or uncooled) allow for better thermal uniformity but are vulnerable to bending strains stemming from time-dependent thermal expansions of the system during the test duration [35], [42]. Nonetheless, the bulk size of wedge grips presents challenges to the physical accessibility of subscale specimen, especially for high temperature setups.

To this point, MTS Advantage™ Mini Grips have been recently developed and are commercially available to address miniature specimen testing concerns around slippage and proper alignment [43]. Advertised miniature specimen geometries compatible with Mini Grips have been previously reported in [10], [11], [30], [44]. The spring-loaded wedge grip mechanism allows for quick, low-force specimen loading that reduces concern for accidental specimen bending. However, the miniature grip system is only suited for room temperature test conditions, and there is no demonstrated intent to adapt the Mini Grips for high temperature environments.

Regardless of gripping method, repeated testing at elevated temperatures may result in oxidation, warpage, and creep of gripping devices and pulls rods that can result in increased bending strains [42]. Thus, periodic verification of alignment is recommended.

3.3 Heating Sources

A range of heating methods can be selected from to achieve high temperature environments for mechanical evaluations. Those commonly implemented are radiant, resistance, and induction heating. Table 3 outlines the general specifications for each method along with their primary benefits and limitations. This section provides a brief overview of each technique.

3.3.1 Radiant Heating

Split ceramic furnaces, which utilize radiant heating, are ubiquitous to high temperature mechanical testing, and are frequently used in subscale testing [14], [16], [21], [41], [45]. Typical systems consist of two-piece ceramic housings outfit with heating element arrays (e.g., resistance heating elements, quartz lamps), one or more viewports for line-of-sight specimen access, and a narrow slit for contact extensometry. Specimens are heated via radiant heat transfer, allowing for greater flexibility with selected specimen geometry and size. Most notably, split furnaces afford excellent temperature control and low thermal gradients in test specimens [41]. Alam et al. [41] used radiant heating via a split-ceramic clamshell furnace to demonstrate excellent thermal control of bowtie-derived subscale specimens within ~5 °C over a 30 mm length (Figure 3). However, limitations consist of sluggish heating and cooling rates due to large thermal inertia [46] and restricted specimen access for instrumentation. Radiant heating often incorporates warm or hot grips that are inside the heating system as heating only a subscale specimen gauge length is difficult.

Table 3. Specifications of Common Heating Methods for High Temperature Tensile Testing.

Heating method	Temperature range	Heating rate	Strengths	Constraints
Radiant	Up to 1600 °C (in air)	20 °C/min (Limited control)	-Direct contact with test specimen -Superior thermal uniformity and stability	-Slow heating rate, poor control due to large thermal inertia -Limited accessibility to specimen
Resistance	>2000 °C	10^3 °C/min	-Rapid heating/cooling -Excellent thermal uniformity and stability -Improved accessibility to specimen	-Specimen geometry dependent -Heating localization during necking -May induce voltages in thermocouples (i.e., erroneous temperatures)
Induction	>2000 °C	10^3 °C/min	-Rapid heating rate -Improved accessibility to specimen -Excellent thermal uniformity and stability	-Material must be susceptible to magnetic field to directly heat -May induce voltages in thermocouples (i.e., erroneous temperatures) -Thermal uniformity can be difficult to achieve -Sensitive to specimen geometry

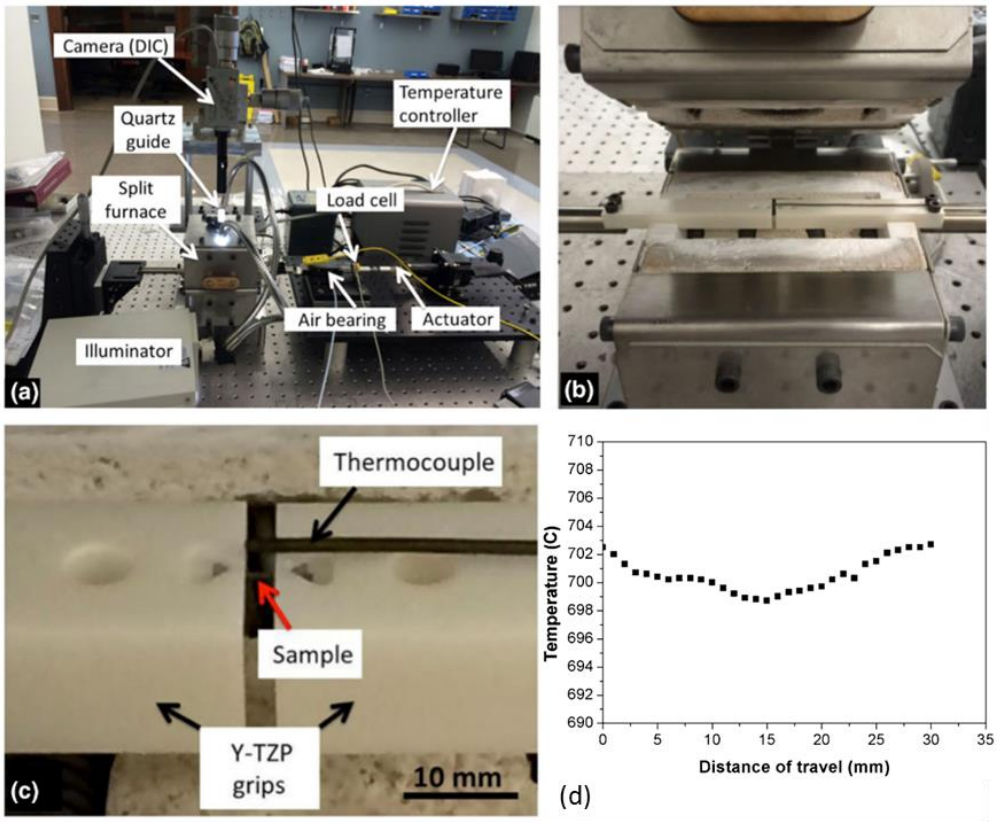

Figure 3. (a) High Temperature Micro-tensile Setup. (b) Split Furnace. (c) Close-up of Ceramic Pull-rods and Bowtie Specimen. (d) Thermal Profile of the Bowtie specimen at 700 °C Target Temperature [41].

3.3.2 Resistance Heating

Alternatively, resistance heating provides a rapid heating method for high temperature testing. Heat generation in this method stems from the natural resistance to the flow of electrons through a material under an applied electrical load. As a result, the material must be electrically conductive to be a candidate. Moreover, numerous studies have successfully performed high temperature subscale testing using an electro-thermal mechanical testing (ETMT) system [21], [47], [48], which is now commercially available through Instron®. Resistance heating also allows for excellent thermal uniformity [19], [49] (Figure 4). However, resistance heating is inherently sensitive to the specimen geometry. As the cross-sectional area narrows during a test, particularly during necking, it leads to a localized increase in resistance which affects temperature uniformity [19], [41]. Furthermore, if thermocouples are used for feedback control, the effects of applied voltages from electrical heating on the thermocouple signals must be accounted for [19]. Despite these drawbacks, resistance heating has demonstrated excellent physical assess to the specimen to perform highly instrumented testing [19].

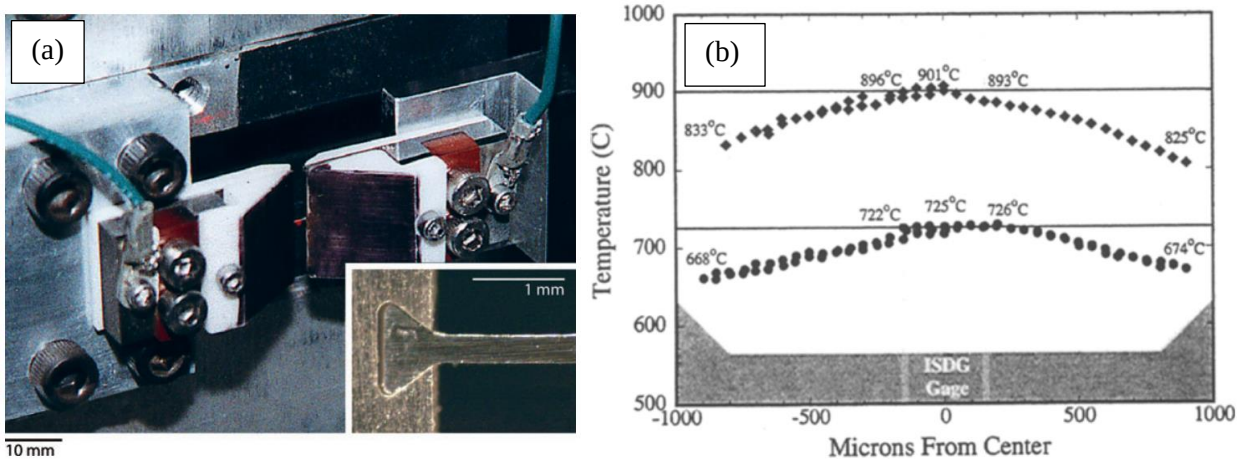

Figure 4. (a) Grips for Elevated Micro-tensile Experiments. Bowtie-shaped Specimens are Held in Self-aligning Grip that are Thermally and Electrically Isolated from the Load Train [50]. (b) Thermal Profile of Bowtie Specimen Along Gauge Length [19].

3.3.3 Induction Heating

Induction heating, which heat specimens through induced eddy currents from exposure to an electromagnetic field, shares many of the same benefits and limitations as resistance heating. First, it is capable of rapid, controlled heating and cooling rates and can achieve excellent thermal gradients with proper set up, inductor design, and/or use of flux concentrating materials. However, it is limited to electrically conductive materials but can be used to indirectly heat non-conductive materials with a susceptor. Moreover, thermal uniformity is highly influenced by specimen geometry (i.e. round versus flat) and specimen thickness, as these geometric parameters affect the skin depth of the current flow, i.e. the imparted thermal gradient [51]. Additionally, design of the inductor geometry plays a critical role in specimen accessibility, particularly for subscale sizes due to physical constraints [51]. Song et al. [52] achieved indirect induction heating of subscale specimens by heating the grips directly and allowing conduction to heat the specimen (

Figure 5) though other implementations focus the field on the specimen gauge length and minimize grip heating. This allowed the authors line-of-sight access to perform interferometric strain measurements [52]. Lastly, another potential limitation is induced voltages can occur when thermocouple wires are exposed to an electromagnetic field [53], which may influence temperature measurements and controls.

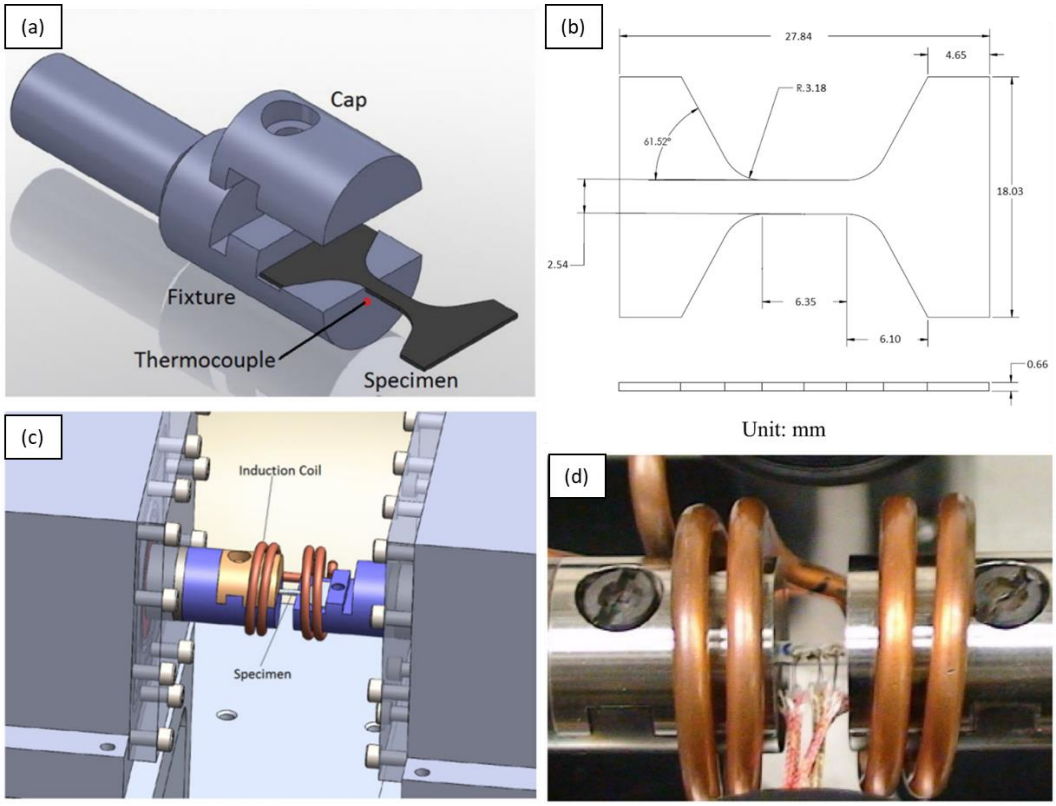

Figure 5. (a) Engineering Model of Pinch-Plate Gripping System. (b) Drawing of Subscale Tensile Specimen Geometry. (c) Engineering Model and (d) Experimental Assembly of Grip and Inductor [52].

3.4 Instrumentation and Measurement

This section reports instrumentation often used to measure and control various aspects of high temperature tensile testing while highlighting subscale geometry-specific challenges.

3.4.1 Temperature

Accurate, timely temperature measurement and control are paramount to the quality of high temperature testing, Generally, these are performed experimentally through contact and non-contact means. Thermocouples welded to the specimen surface offer temperature measurements over 2000 °C, errors of ≤1%, and instantaneous signal feed-back for closed-loop heating control [54]. Furthermore, thermocouples offer an effective way to characterize thermal gradients in experimental setup validation [19]. However, one limitation when welding thermocouples, especially for subscale specimens, is local alteration of microstructure, which could affect performance [19] and could wick heat from the specimen – affecting the measurement. One possibility to circumvent this issue is to weld the thermocouple to the gauge section fillet of the specimen. Yet, this methodology only works if the specimen and system are in thermal equilibrium at the time testing. Heating methods, such as induction heating, may impart a transient thermal response, causing the control temperature to drift erroneously as the system and specimen thermally evolve during testing. Additionally, thermocouple accuracy may be compromised in the presence of electrical current [19] and electromagnetic fields [53] that are found in resistance and induction heating methods, respectively.

Alternatively, non-contact temperature methods avoid many of complications associated with contact techniques. One popular method is infrared pyrometry, which measures emitted thermal radiation to determine temperature [19], [23], [41], [55], [56]. This technique offers a broad temperature measurement range of over 3500 °C [57]. Spot sizes are often approximately 1-3 mm in diameter, leading to localized, point-source temperature measurements. Importantly, emissivity, which is the ratio of the emitted radiant energy of an object to a blackbody at the same temperature, must be considered for accurate temperature measurements since emissivity is a function of geometry of the radiative surface (i.e. surface roughness), temperature, and wavelength [58].

Single wavelength (or color) pyrometers are the simplest and relatively inexpensive configuration but require knowledge of the spectral emissivity for a given material to accurately compensate temperature measurements. However, metallic materials in air environments at high temperature readily oxide, altering the spectral emissivity over the duration of a test [59], which complicates measurement fidelity. Moreover, single wavelength pyrometers are sensitive to line-of-sight obstructions, such as smoke, dust, and dirtied optical windows. In all, if the physical and optical properties of the target material are well understood, single wavelength pyrometers are a viable option.

Two-color (or ratio) pyrometers seek to circumvent challenges with emissivity corrections by using two wavelengths. In theory, by using the ratio of radiance intensity at two close wavelengths, the associated emissivities would cancel out in division. However, the ratios of the spectral emissivities often vary with temperature and lead to large errors in temperature measurement accuracy, and thus are largely avoided unless dealing with obfuscated line-of-sight for the target [57].

To improve upon the shortcomings of two-color pyrometer, multi-band pyrometers have been developed to utilize additional wavelength bands to reduce the dependency of the measurement on *a priori* knowledge of material emissivity and to produce highly accurate temperature measurements within the uncertainty bounds of a reference thermocouple (<1%) [60].

3.4.2 Strain

Strain measurements for high temperature testing are comprised of contact and non-contact techniques. A summary of commonly used techniques is shown in Table 4. However, this report will emphasize two of those most frequently utilized: linear variable differential transformer (LVDT) and digital image correlation (DIC).

Table 4. Advantages and Disadvantages of Some Candidate Strain and Displacement Measurement Techniques for Miniaturized Test Systems. Adapted from [21].

Techniques	Advantages	Disadvantages
LVDT (linear transducers)	Readily available, sub micrometre resolution point displacement.	Measures displacement cf. strain, requires point contact.
Electrical resistance	Cheap and direct method with simple analysis to provide plastic strain values. Excellent at high temperatures right up to solidus.	Only possible with electrically conducting materials. Only measures plastic strain values. Requires additional calibration if phase changes occur during the test to alter intrinsic resistivity values.
Capacitance gauges	High resolution displacement measurement.	Average displacement measurement, requires some physical contact, drift.
Line scan cameras	Cheap, high resolution measurement.	Two-dimensional mapping only possible with a scanning system.
Laser interferometry	High resolution displacement and strain measurement (5 με).	Reflective targets required. Sensitive to vibration and rigid body motion.
Digital speckle pattern interferometry	Full field, non-contact, measurement. High sensitivity and spatial resolution. Two- and three-dimensional measurement capability. High temperature capability.	Expensive, sensitive to vibration. Requires a diffuse surface. Not suitable for large deformations or rigid body motion.
Digital image correlation	Full field, non-contact, two- and three-dimensional implementations available, wide range of cameras and suppliers. Can be used on SEM images.	Modest strain resolution (0·01 pixel/100 με) depending on camera resolution and field of view, testpiece may require some surface pattern or preparation.
Photoelastic stress analysis	Full field, non-contact, direct measurement of stress and strain.	Photoelastic coatings must be applied. Limited temperature range, stress level may saturate.

High temperature LVDT, capacitive, or strain gauge extensometers are outfit with alumina or SiC rods for direct contact with the specimen for testing up to 1200-1600 °C. These contact methods offer superior sub-micron resolution and enable simultaneous data collection and feedback control for strain-controlled measurements. However, one limitation is physical access with decreasing specimen size and a greater impact of knife edge radius on determining the actual gauge length of the extensometer. Commercially available products offer 10 mm gauge lengths as a minimum size so custom instrumentation much be generated for achieving anything smaller. Additionally, for very small material volumes, surface contact with the rods can act as

thermal heatsinks, which generate thermal nonuniformity. This is most prevalent for induction and resistance heating since the bulk of the ceramic rods remain at room temperature.

DIC has emerged as an effective non-contact method for full-field displacement and strain determination during material deformation in either two- or three-dimensions. In its most basic form, the setup requires oblique-angled light sources for illumination, a digital camera, magnifying optics, and a computer for image processing [61]. The specimen requires sufficient surface texture or a high-contrast speckle pattern to track displacements and calculate strains through changes in pixel intensity gradients at subpixel resolution [61]. Practiced skill is required to repeatedly apply an optimal speckle to specimens [62], [63]. In addition, cross-polarization techniques enhances pattern contrast, resulting in better resolution and reduced pixel noise [64]. Furthermore, the scale-invariant nature of DIC is one of its best strength, which makes it highly suited for subscale tensile testing [11], [28]. For instance, Gussev et al. [10] utilized DIC to assess the viability of three different subscale tensile specimen geometries. The implementation of DIC allowed for a precise comparison by filtering out grip-associated plastic strain inaccuracies that would have otherwise skewed perceived performance [10]. Moreover, other researchers have utilized DIC to accurately measure the constitutive response of irradiated steels from subscale specimen tests [12], [65]. However, DIC for subscale testing is largely performed at room temperature.

For high temperature testing, there are three primary challenges that plague the use of DIC: 1) image saturation from thermal radiation of heat specimens and surroundings; 2) loss of image contrast due to surface oxidation and/or speckle pattern degradation; 3) image distortion from heat haze. Thermal radiation effects stem from the fact that any object above zero Kelvin emits electromagnetic waves. As specimens are heated for testing, they begin to emit light at wavelengths in the visible spectrum. This leads to a reduction in image contrast and jeopardizes the quality of the DIC analysis [66], as shown in Figure 6. Researchers [66]–[69] have found that the use of blue or UV light for illumination, coupled with bandpass filters, largely mitigates the contributions from blackbody thermal radiation to image grayscale pixel intensity. An example of image contrast stability from blue and UV light and bandpass filters is shown in Figure 7. Image contrast loss can also originate from oxidation of the specimen surface and/or the speckling media itself. Moreover, oxidative and thermal effects can lead to debonding, cracking, or peeling of the speckling media [62]. Recent efforts have identified a list of thermally-stable oxides and carbides capable of pushing the operable range of the technique upwards of 3000 °C [70]. In addition, the application of speckle media may also react with and damage the specimen surface with complicate use in high temperature applications. Lastly, heat haze effects can lead to large amounts of pixel noise or even speckle decorrelation [70]. The observed image distortions are caused by gradients in the refractive index of the air near a heated specimen. Methods identified to minimize the effects include testing in vacuum [68], use of an air knife [56], and image processing techniques such as an average approach and prolonged exposure time [70], or quite recently, application of deep learning models [71].

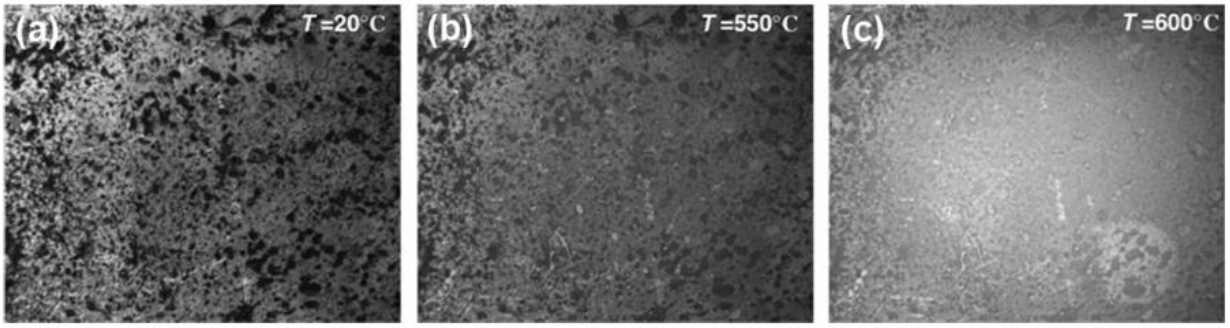

Figure 6. Recorded Images of the Surface of a Stainless Steel Sample Using a Conventional Optical Imaging System at Temperatures of (a) 20, (b) 550 and (c) 600 °C [66].

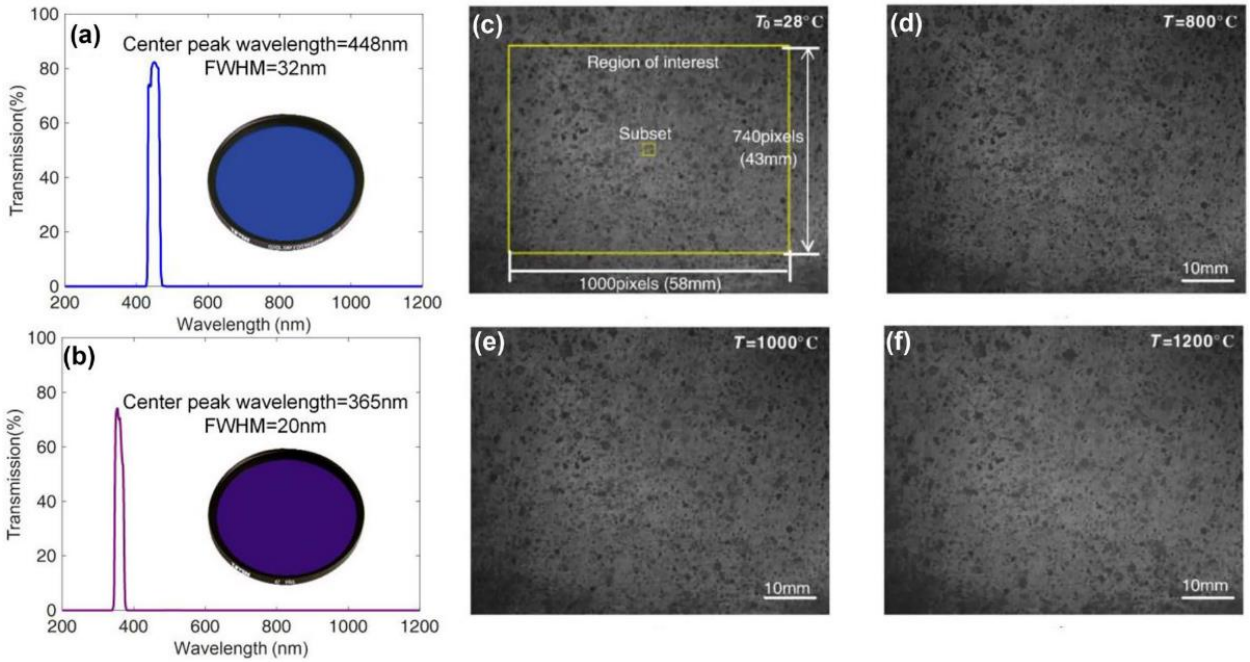

Figure 7. Transmission Spectrum of (a) a Blue Filter and (b) a UV Filter. Recorded Images of the Surface of a Stainless Steel Sample Using a Blue-light DIC System at Temperatures of (c) 28, (d) 800, (e) 1000 and (f) 1200 °C [66].

4.0 DISCUSSIONS AND CONSIDERATIONS

This section provides discussion on the presented high temperature testing methods in Section 3.0, as well as addresses considerations specific to the mechanical evaluation of AM materials and components.

4.1 Identified Gaps in Subscale High Temperature Tensile Testing

Generally, the fundamental methods for heating, temperature control, and strain measurements have remained relatively constant over the years for high temperature tensile testing, even for subscale specimens.

The most substantial advancements have come in non-contact strain measurements made possible by technological developments in digital cameras and computing capabilities [57], [72]. On-the-fly image processing allows for real-time strain-control feedback via DIC with comparable sensitivity to traditional contact extensometers [66], [68], [69]. As previously mentioned, the scale-invariant nature of DIC strongly suits the technique for subscale testing, especially at high temperatures. Recent developments in high temperature DIC reported in Section 3.4.2 have enabled the successful application of non-contact strain measurements at extreme temperatures. For example, Pan et al. [67] demonstrated accurate thermal strain measurements of tungsten at over 3000 °C. Furthermore, Yu et al. [68] developed and experimentally validated a high-temperature video extensometer capable of measuring the tensile performance of select refractory alloys up to 2000 °C.

Additionally, as stated in Section 3.4.2, application of artificial speckling media can be problematic via speckle degradation and decorrelation or deleterious interaction with the test material. An alternative method for generating speckling is by using lasers to illuminate an optically rough surface with coherent light. In conjunction with proper filtering optics, this can produce a high-contrast imaging condition for DIC with proven ability to measure high temperature full-field strain maps of ceramic matrix composites and C/C composites at over 1300 °C [73], [74]. This technique is directly applicable for measuring high temperature strain of AM metallic materials, particularly when the as-built surface is retained. The natural surface topology of the as-built surface, when illuminated by a laser, theoretically should produce a high-quality speckle pattern for DIC analyses. Nonetheless, as test temperature and subscale specimen requirements limit the practicality of physical strain measurement, it will be imperative to continue development of DIC techniques to operate in the requisite conditions.

Another limitation is with non-contact thermal measurement capabilities. Pyrometry is widely used to effectively measure and control the temperature feedback loop. However, as previously reported, limitation with single wavelength and dual wavelength units. Moreover, for a research and development facility, new materials are commonly tested and accurate knowledge of the emissivity of developmental alloys and their oxides is limited. Yet, pyrometry requires this knowledge to accurately compensate temperature measurements for real, non-blackbody materials. Thus, it is desirable to have active emissivity compensation capabilities integrated with the temperature measurement instruments. Presently, reliable hardware for measuring emissivity-correct temperature is not commercially available to the best knowledge of the author. Particularly for AM materials, emissivity is not only dependent upon material and temperature, but also upon surface finish [75]. Temperatures measured from a specimen with a specular,

reflective surface versus a diffuse, matte surface will vary dramatically. To this point, measuring the temperature of as-built AM materials will require additional due-diligence to ensure accuracy. Hence, as it stands, there is no "one-size-fits-all" solution for reliable and accurate temperature measurement by non-contact means.

4.2 Effect of Specimen Size on Tensile Properties

As specimen dimensions decrease, it is of utmost importance to consider its effects on tensile performance. Generally, there are geometric aspect ratio requirements that bound the onset of size-dependent response in flat specimens, as summarized in Table 5. These ratios include thickness to grain size (*t/d*), width to thickness (*w/t*), and gauge length to square root of area ($L/\sqrt{A}$) [7], and originate from specimen design guidance issued in ASTM E8 and ISO 6892-1 standards. Below the suggested minimums, the size effects most notably influence tensile response by affecting strain hardening and necking behaviors. Ratios of *t/d* below ~6-10 begin to exhibit dislocation interaction and annihilation at the specimen surface, which decreases the strain hardenability by limiting dislocation multiplication and interaction and leads to reduced elongation [76]. Moreover, increasing ratios of *w/t* beyond a value of ~5 can result in a transition from diffuse to localized necking behavior, which leads to a decrease post-necking elongation [77]. Similarly, increasing the $L/\sqrt{A}$ ratio past 5.65 reduces the volume of the necking region relative to the gauge length, which in turn reduces the amount of post-necking elongation [78].

In conclusion, the smallest dimension of specimen (thickness or diameter) is generally the primary factor for ensuring polycrystalline bulk behavior, while the other dimensions usually relate to the necking behavior and change of total elongation. When specimen dimensions are further reduced to fall outside the suggested limits, subscale testing can lead to large scatter in mechanical test data as performance deviates from representative bulk response.

Table 5. Summary of Size Effects for Flat Specimen Geometries [7].

Dimension	The critical value (the value suggested)	Properties that are affected (under critical value for *t* or *w*)	Dominant mechanism
Thickness (*t*)	$\frac{t}{d}$ (6 – 10)	$\sigma_s, \sigma_u, e_u, e_p, e_f$	surface effects
Width (*w*)	$\frac{w}{t}$ (5)	σ_u, e_p, e_f	necking behavior
Gauge length (*L*)	$\frac{L}{\sqrt{A}}$ (5.65)	e_p, e_f	Bertella-Oliver formula

Where σ_s, σ_s, are yield strength and ultimate tensile strength, respectively. σ_u, σ_p, σ_f are uniform elongation, post-necking elongation, and total elongation, respectively.
A is the cross-sectional area of the specimen and *L* is the original gauge length.

4.3 Considerations for Additive Manufacturing

This section highlights tensile testing considerations specific to AM. While high temperature testing of subscale specimens is unmentioned explicitly, the challenges listed are pervasive to the topic area and need consideration prior to high temperature testing efforts.

4.3.1 Impact of As-built Surface Finishes on Performance Assessment

It is well known that as-built surface finish of AM parts can affect performance. One critical consideration for evaluation of AM tensile specimens, particularly subscale and thin-walled geometries, is how to accurately measure the true load-bearing cross-sectional area. Tilson and Katsarelis [79] directly compared several common measurement techniques for the determination of the nominal cross-sectional area. The authors concluded a clear bias to overestimate the area when using calipers, ball mics, and point mics by as much as 15% [79]. The results showed that destructive area measurements minimized tensile strength variability for test specimen thicknesses between 0.5 mm and 2.54 mm, suggesting nearly all the performance discrepancy originated from the metrology [79]. What's more, Yu et al. [80] found that size-dependent effects from varying specimen thickness were minimal if surface roughness measurements are properly accounted for. The authors determined that the overestimation of nominal area using caliper measurements was compensated using maximum profile peak height, $R_{p,}$ from metallographic cross-sections. Moreover, Roach et al. [25] examined the tensile response of five different proportionally scaled specimen geometries. Despite little variation in the intrinsic microstructure and microhardness between the specimen sizes, strength and modulus were observed to decrease with decreasing specimen size. The authors concluded the as-built surface roughness obfuscated the determination of the true load-bearing area for the specimens. As specimen surface area to volume ratios decreased, specimen performance was found to approach bulk properties [25]. Thus, this highlights a clear debit that exists when 3D-printed feature sizes decrease since surface roughness can significantly alter the specimen geometry, and more importantly, performance. Furthermore, for brittle metallic alloys, geometry-dependent surface roughness can originate stress concentrators that may significantly impact performance, as well [25]. Ultimately, questions remain for how to 1) rapidly, accurately, and non-destructively quantify surface roughness and 2) incorporate a correction factor into performance determination. All of this to say, there is a need for universally accepted methodologies for measuring the true load-bearing cross-sectional area of subscale and thin-walled AM specimens with as-built surface finishes.

4.3.2 Intrinsic Versus Extrinsic Performance of AM Metallic Materials

To continue the considerations discussed in Section 4.3.1, it is imperative for researchers to clearly define the material-related question probed through tensile testing of AM metallic materials. For instance, researchers often strive to understand the intrinsic material responses for modeling and predictive capabilities. This requires the assessed material to be defect-free and have an acceptable low-stress, machined surface finish. However, AM parts often retain as-built surface roughness and inherent volumetric defects (e.g., cracks, lack-of-fusion, and keyhole porosities), which diminish overall performance. This introduces a new wrinkle into predictive intrinsic material models that may not capture real-world performance due to AM process-induced flaws. This begs the question: what material properties are most relevant for AM materials – intrinsic or extrinsic? Given sufficiently low surface area to volume ratios and

relatively defect-free test specimens, intrinsic or "bulk" material properties are measurable in AM materials [25]. However, when considering AM thin-walled geometries, the argument could be made that extrinsic performance is most important due to stress concentrators on the surface, as discussed by Roach et al. [25]. Boyce et al. [81] sought to use extreme value statistics to develop probabilistic model-based correlations for reliability due to the inherent difficulty in predicting AM process variability. The study analyzed over 1000 nominally identical AM tensile tests to reveal ~2% of the test population was afflicted by rare porosity defects that substantially diminished ductility. Summarily, it is vitally important to understand the best approach for performance assessment and modeling for AM part-specific applications as geometric features and specimen sizes are reduced.

4.3.3 Current Utilization of Subscale Tensile Geometries in AM

The development and performance analysis of AM processes is poised to benefit from subscale testing when material availability is limited or cost prohibitive. Watring et al. [13], [29] examined tensile performance of AM Inconel 718 from subscale specimens excised from the grip sections of previously tested standard-sized fatigue specimens. In the case for laser powder-bed fusion, AM also affords the ability to directly print tensile specimens. Heckman et al. [33] utilized a bowtie-derived subscale specimens to develop a stochastic model of process parameter sensitivity using automated high-throughput tensile testing of AM 316L stainless steel. It should be pointed out that the print dimensional variation in the grip end of the bowtie specimen can affect the specimen alignment and measured performance. Other studies have taken more traditional approaches to produce subscale specimens from basic rectangular prism blanks of AM material in order to perform characterization [31], [32].

What's more, AM components may contain geometric features, e.g., thin walls, overhangs, intersections, etc., that require site-specific investigation. This concept has been recently demonstrated by Džugan et al. [30] who used miniature specimens to evaluate local tensile properties and fracture behavior of AM Inconel 718 in the as-built and heat treated conditions. Moreover, Džugan et al. [44] used micro-tensile specimens to analyze site-specific performance of a L-PBF IN718 jet turbine blade, an EB-PBF Ti-6Al-4V propeller, and a L-PBF H13 tool steel propeller. Tensile results showed discernable differences in yield strength (YS) and ultimate tensile strength (UTS) for various site-specific tests [44] that otherwise go uncaptured in traditional materials-based performance models.

Nonetheless, questions remain for how to feasibly assess quality and performance in AM parts. As mentioned, it can be costly and time consuming to excise specimens from finished components, especially if the final parts are of appreciable volume. The use of witness coupons has been broached to solve this dilemma through the development of standards and guidelines for AM build qualification [82]–[84]. However, ASTM E8 standard and subsize specimens are often prescribed for evaluation testing, which, due to the relatively large size, fail to capture thin-walled feature performance debits. Recently, researchers have sought to embody all relevant AM build features in a single, universally designed test artifact [85] but a generalized approach to witness coupon design may be better suited [86], [87], as the design space for AM components is expansive. Moreover, as integrated computation materials engineering (ICME) tools continually improve, their utilization may allow for proper witness coupon design by tailoring the coupon geometry to mimic the RVE of the AM feature in question based on processing conditions.

Nonetheless, in general, witness coupons must capture a representative volume element (RVE) of microstructure, thermal history, and surface finish for the feature of inquiry. In certain instances when witness coupons are of similar geometric form and in close proximity to the site-specific test of interest, it has been shown that witness coupons can accurately capture YS and UTS properties within 5% of site-specific micro-tensile tests [44]. While promising, the reliability of witness coupons should be judiciously approached and developed on a part-specific basis as to avoid misleading results [88], [89].

5.0 CONCLUSIONS

The guiding principles for tensile testing of standard specimens are generally the same for subscale specimen. Test setup must be given additional scrutiny for assessment of imposed strains from system misalignment and gripping, especially at higher test temperatures. Efforts are currently underway to standardize guidelines for subscale tensile testing at room temperature and to develop an AM-relevant rectangular tensile specimen geometry by ASTM Subcommittees E28.04.01 and F42.01, respectively. A bowtie specimen geometry with pull-rod gripping was the most observed high temperature tensile testing setup for subscale specimens.

When material is limited in quantity or size, subscale tensile specimens can accurately characterize bulk response, though reports of testing at elevated temperatures are limited. Size-dependent effects must be considered when using subscale specimen geometries. Generally, it has been shown that YS and UTS are intensive properties while elongation is highly sensitive to thickness and gauge length. To ensure polycrystalline bulk behavior, on average, the minimum cross-sectional dimension should comprise of at least 10 grains, the width is 5 times the thickness, and the gauge length should be 5.65 times as long as the square root of the area for elongation. Moreover, while an array of subscale specimen geometries has been reported, they are generally flat and are derived from SSJ-series and SS-series geometries.

Elongation is highly influenced by gauge length and specimen thickness, particularly post-necking. Special consideration should be given to design of subscale specimen if total elongation data are needed. Implementation of inverse finite element methodologies to model post-necking elongation to failure may be utilized.

Recent advancements in non-contact methods, e.g., video extensometry and DIC, can allow for real-time analysis of high-resolution strain measurements at extreme temperatures. The scale-invariant nature of the techniques strongly complements subscale tensile testing.

Accurate temperature measurement and control are arguably the most challenging aspects of high temperature testing. There are clear trade-offs between contact and non-contact methodologies through the potential to alter locally the microstructure with welded thermocouples or the emissivity-related challenges for pyrometry. Moreover, these challenges may be exacerbated by as-built surface roughness in AM metallic materials.

6.0 RECOMMENDATIONS

As specimen size and nominal thickness decrease, RVEs of the microstructure have increasing impact on the performance. Sufficient microstructural feature populations based upon grain size, texture, and phase distribution are critical to accurately represent performance of a particular structure, regardless of test temperature. As such, critical thought must be given to the specimen geometry selected for analysis.

It is recommended that instrumentation for non-contact measurements and techniques utilizing the technology continue to be developed. Presently, subscale tensile testing and high temperature DIC techniques are reported independently of each other. Efforts are needed to integrate the test methods to overcome contact strain measurement limitations (i.e., thermal losses, constrained accessibility) as specimen geometries miniaturize. Furthermore, DIC generates full-field strain measurements that can capture heterogeneous, localized deformation phenomena unlike conventional strain measurements. This may also be of interest for tensile testing under thermal gradients where spatially dependent constitutive response is expected. In addition, continued development of non-contact thermal measurement instruments that can account for evolving emissivity *in-situ* will mitigate errors associated with changes in surface topology and chemical composition (i.e., oxidation). What's more, many commercially available pyrometers only have >2 mm spot sizes. Development of optics to enable sub-millimeter spot sizes is needed for subscale specimen geometries.

Given the discussion around cross-sectional measurement uncertainty in AM test specimens, it is recommended that a rapid and accurate non-destructive method be developed to measure true load-bearing cross sectional area for thin-walled AM features in which surface roughness accounts for appreciable error in stress calculations.

Measurement variability for tensile properties increases as geometric critical design limits are approached. For certain applications, especially involving AM materials, the targeted feature size can include thin-walled geometries and as-built surfaces. These features contain inherent process variability, and large datasets are needed to capture stochastic response for extreme-value probabilistic performance modeling. Thus, it is desirable to design high-throughput methodologies to screen tensile properties of AM materials at high temperatures. Non-contact instrumentation will be critical to this effort.

Lastly, the reviewed subscale specimen geometries have demonstrated the ability to capture bulk tensile response given their design exceeds critical limits with respect to gauge length, width, and thickness. Presently, no standard subscale tensile specimen geometries exist, but it is recommended current standardization efforts continue as to provide acceptable design guidelines and considerations.

7.0 REFERENCES

[1] Y. Zhu and H. D. Espinosa, "An electromechanical material testing system for in situ electron microscopy and applications," *Proc. Natl. Acad. Sci. U. S. A.*, vol. 102, no. 41, pp. 14503–14508, 2005, doi: 10.1073/pnas.0506544102.

[2] D. Kiener and A. M. Minor, "Source truncation and exhaustion: Insights from quantitative in situ TEM tensile testing," *Nano Lett.*, vol. 11, no. 9, pp. 3816–3820, 2011, doi: 10.1021/nl201890s.

[3] G. D. Sim, J. H. Park, M. D. Uchic, P. A. Shade, S. B. Lee, and J. J. Vlassak, "An apparatus for performing microtensile tests at elevated temperatures inside a scanning electron microscope," *Acta Mater.*, vol. 61, no. 19, pp. 7500–7510, 2013, doi: 10.1016/j.actamat.2013.08.064.

[4] W. D. Summers, E. Alabort, P. Kontis, F. Hofmann, and R. C. Reed, "In-situ high-temperature tensile testing of a polycrystalline nickel-based superalloy," *Mater. High Temp.*, vol. 33, no. 4–5, pp. 338–345, 2016, doi: 10.1080/09603409.2016.1180857.

[5] M. L. Taheri *et al.*, "Current status and future directions for in situ transmission electron microscopy," *Ultramicroscopy*, vol. 170, no. Bâtiment MXC, pp. 86–95, 2016, doi: 10.1016/j.ultramic.2016.08.007.

[6] P. Hosemann, "Small-scale mechanical testing on nuclear materials: bridging the experimental length-scale gap," *Scr. Mater.*, vol. 143, pp. 161–168, 2018, doi: 10.1016/j.scriptamat.2017.04.026.

[7] P. Zheng *et al.*, "On the standards and practices for miniaturized tensile test – A review," *Fusion Eng. Des.*, vol. 161, no. September, p. 112006, 2020, doi: 10.1016/j.fusengdes.2020.112006.

[8] H. Liu, Y. Shen, S. Yang, P. Zheng, and L. Zhang, "A comprehensive solution to miniaturized tensile testing: Specimen geometry optimization and extraction of constitutive behaviors using inverse FEM procedure," *Fusion Eng. Des.*, vol. 121, pp. 188–197, 2017, doi: 10.1016/j.fusengdes.2017.07.016.

[9] L. S. Moura *et al.*, "A highly accurate methodology for the prediction and correlation of mechanical properties based on the slimness ratio of additively manufactured tensile test specimens," *J. Mater. Sci.*, vol. 55, no. 22, pp. 9578–9596, 2020, doi: 10.1007/s10853-020-04654-y.

[10] M. N. Gussev, R. H. Howard, K. A. Terrani, and K. G. Field, "Sub-size tensile specimen design for in-reactor irradiation and post-irradiation testing," *Nucl. Eng. Des.*, vol. 320, pp. 298–308, 2017, doi: 10.1016/j.nucengdes.2017.06.008.

[11] J. Džugan, R. Procházka, and P. Konopík, "Micro-tensile test technique development and application to mechanical property determination," *ASTM Spec. Tech. Publ.*, vol. STP 1576, pp. 12–30, 2015, doi: 10.1520/STP157620140022.

[12] H. Liu *et al.*, “True stress-strain curve extraction from ion-irradiated materials via small tensile, small punch and nanoindentation tests: Method development and accuracy/consistency verification,” *Nucl. Fusion*, vol. 60, no. 5, 2020, doi: 10.1088/1741-4326/ab7c2a.

[13] D. S. Watring, J. T. Benzing, N. Hrabe, and A. D. Spear, “Effects of laser-energy density and build orientation on the structure–property relationships in as-built Inconel 718 manufactured by laser powder bed fusion,” *Addit. Manuf.*, vol. 36, no. February, p. 101425, 2020, doi: 10.1016/j.addma.2020.101425.

[14] J. Schulthess, R. Lloyd, B. Rabin, M. Heighes, T. Trowbridge, and E. Perez, “Elevated temperature tensile tests on DU-10Mo rolled foils,” *J. Nucl. Mater.*, vol. 510, pp. 282–296, 2018, doi: 10.1016/j.jnucmat.2018.08.024.

[15] J. Lin and C. Liang, “Investigations of high-temperature tensile properties temperature Pb-free solders,” *J. Mater. Sci. Mater. Electron.*, vol. 31, no. 21, pp. 19318–19331, 2020, doi: 10.1007/s10854-020-04466-5.

[16] E. M. Fayed, M. Saadati, D. Shahriari, and V. Brailovski, “Effect of homogenization and solution treatments time on the elevated - temperature mechanical behavior of Inconel 718 fabricated by laser powder bed fusion,” *Sci. Rep.*, no. 0123456789, pp. 1–17, 2021, doi: 10.1038/s41598-021-81618-5.

[17] K. Kumar *et al.*, “Use of miniature tensile specimen for measurement of mechanical properties,” *Procedia Eng.*, vol. 86, pp. 899–909, 2014, doi: 10.1016/j.proeng.2014.11.112.

[18] K. Kumar, A. Pooleery, K. Madhusoodanan, and R. N. Singh, “Optimisation of thickness of miniature tensile specimens for evaluation of mechanical properties Materials Science & Engineering A Optimisation of thickness of miniature tensile specimens for evaluation of mechanical properties,” *Mater. Sci. Eng. A*, vol. 675, no. August, pp. 32–43, 2016, doi: 10.1016/j.msea.2016.08.032.

[19] M. Zupan, M. J. Hayden, C. J. Boehlert, and K. J. Hemker, “Development of high-temperature microsample testing,” *Exp. Mech.*, vol. 41, no. 3, pp. 242–247, 2001, doi: 10.1007/BF02323140.

[20] D. W. Eastman *et al.*, “Benchmarking crystal plasticity models with microtensile evaluation and 3D characterization of René 88DT,” *Proc. Int. Symp. Superalloys*, vol. 2016-Janua, pp. 813–820, 2016, doi: 10.1002/9781119075646.ch87.

[21] J. D. Lord, B. Roebuck, R. Morrell, and T. Lube, “25 year perspective: Aspects of strain and strength measurement in miniaturised testing for engineering metals and ceramics,” *Mater. Sci. Technol.*, vol. 26, no. 2, pp. 127–148, 2010, doi: 10.1179/026708309X12584564052012.

[22] S. Holmström, M. Bruchhausen, and K.-F. Nilsson, *Test methodologies for determining high temperature material properties of thin walled tubes EERA JPNM Pilot project TASTE*. 2017.

[23] K. J. Hemker and W. N. Sharpe, “Microscale characterization of mechanical properties,” *Annu. Rev. Mater. Res.*, vol. 37, no. February, pp. 92–126, 2007, doi: 10.1146/annurev.matsci.36.062705.134551.

[24] D. A. LaVan and W. N. Sharpe, “Tensile testing of microsamples,” *Exp. Mech.*, vol. 39, no. 3, pp. 210–216, 1999, doi: 10.1007/BF02323554.

[25] A. M. Roach, B. C. White, A. Garland, B. H. Jared, J. D. Carroll, and B. L. Boyce, “Size-dependent stochastic tensile properties in additively manufactured 316L stainless steel,” *Addit. Manuf.*, vol. 32, no. January, p. 101090, 2020, doi: 10.1016/j.addma.2020.101090.

[26] G. Partheepan, D. K. Sehgal, and R. K. Pandey, “An inverse finite element algorithm to identify constitutive properties using dumb-bell miniature specimen,” *Model. Simul. Mater. Sci. Eng.*, vol. 14, no. 8, pp. 1433–1445, 2006, doi: 10.1088/0965-0393/14/8/010.

[27] J. Džugan, P. Konopik, M. Rund, and R. Prochazka, “Determination of Local Tensile and Fatigue Properties With the Use of Sub-Sized Specimens,” in *Volume 1A: Codes and Standards*, Jul. 2015, pp. 1–8, doi: 10.1115/PVP2015-45958.

[28] M. N. Gussev, J. T. Busby, K. G. Field, M. A. Sokolov, and S. E. Gray, “Role of scale factor during tensile testing of small specimens,” in *Small Specimen Test Techniques: 6th Volume*, vol. STP 1576, 100 Barr Harbor Drive, PO Box C700, West Conshohocken, PA 19428-2959: ASTM International, 2014, pp. 31–49.

[29] D. S. Watring *et al.*, “Evaluation of a modified void descriptor function to uniquely characterize pore networks and predict fracture-related properties in additively manufactured metals,” *Acta Mater.*, vol. 223, p. 117464, 2022, doi: 10.1016/j.actamat.2021.117464.

[30] J. Dzugan, M. Seifi, M. Rund, P. Podany, R. Grylls, and J. J. Lewandowski, “The Use of Miniature Specimens to Determine Local Properties and Fracture Behavior of LPBF-Processed Inconel 718 in as-Deposited and Post-Treated States,” *Materials (Basel).*, vol. 15, no. 13, 2022, doi: 10.3390/ma15134724.

[31] M. R. Gotterbarm *et al.*, “Small scale testing of IN718 single crystals manufactured by EB-PBF,” *Addit. Manuf.*, vol. 36, no. July, p. 101449, 2020, doi: 10.1016/j.addma.2020.101449.

[32] J. Benzing, N. Hrabe, T. Quinn, R. White, R. Rentz, and M. Ahlfors, “Hot isostatic pressing (HIP) to achieve isotropic microstructure and retain as-built strength in an additive manufacturing titanium alloy (Ti-6Al-4V),” *Mater. Lett.*, vol. 257, p. 126690, 2019, doi: 10.1016/j.matlet.2019.126690.

[33] N. M. Heckman *et al.*, “Automated high-throughput tensile testing reveals stochastic process parameter sensitivity,” *Mater. Sci. Eng. A*, vol. 772, no. October 2019, p. 138632, 2020, doi: 10.1016/j.msea.2019.138632.

[34] “Tensile Testing: An Introduction,” *Instron*, 2023. https://www.instron.com/en/resources/test-types/tensile-test (accessed Feb. 09, 2023).

[35] M. STEEN and J. BRESSERS, *Alignment: a critical issue in high temperature testing*. Woodhead Publishing Limited, 1995.

[36] ASTM Interational, ASTM E1012-19: “Standard practice for verification of testing frame and specimen alignment under tensile and compressive axial force application," 2019.

[37] ASTM International, ASTM E21-20: “Standard Test Methods for Elevated Temperature Tension Tests of Metallic Materials, ASTM International,” 2020.

[38] S. Dryepondt, P. Nandwana, P. Fernandez-Zelaia, and F. List, “Microstructure and high temperature tensile properties of 316L fabricated by laser powder-bed fusion,” *Addit. Manuf.*, vol. 37, no. October 2020, p. 101723, 2021, doi: 10.1016/j.addma.2020.101723.

[39] S. Karnati, I. Axelsen, F. F. Liou, and J. W. Newkirk, “Investigation of tensile properties of bulk and SLM fabricated 304L stainless steel using various gage length specimens,” *Solid Free. Fabr. 2016 Proc. 27th Annu. Int. Solid Free. Fabr. Symp. - An Addit. Manuf. Conf. SFF 2016*, pp. 592–604, 2016.

[40] D. S. Gianola and C. Eberl, “Micro- and nanoscale tensile testing of materials,” *Jom*, vol. 61, no. 3, pp. 24–35, 2009, doi: 10.1007/s11837-009-0037-3.

[41] Z. Alam, D. Eastman, M. Jo, and K. Hemker, “Development of a High-Temperature Tensile Tester for Micromechanical Characterization of Materials Supporting Meso-Scale ICME Models,” *Jom*, vol. 68, no. 11, pp. 2754–2760, 2016, doi: 10.1007/s11837-016-2100-1.

[42] C. G. LARSEN, L. E. JOHNSON, and L. G. MOSIMAN, *Gripping techniques and concerns for mechanical testing of ultra high temperature materials*. Woodhead Publishing Limited, 1995.

[43] MTS Systems, “MTS Advantage™ Mini Grips,” 2021, [Online]. Available: https://www.mts.com/-/media/materials/pdfs/brochures/mts-advantage-mini-grips-brochure.pdf?as=1 (accessed Feb. 9, 2023).

[44] J. Dzugan *et al.*, “Mechanical properties characterisation of metallic components produced by additive manufacturing using miniaturised specimens,” *Virtual Phys. Prototyp.*, vol. 18, no. 1, 2023, doi: 10.1080/17452759.2022.2161400.

[45] S. Dmas, V. Bonnand, J.-B. le Graverend, and M. Bartsch, “Mechanical characterization at high temperature,” in *Nickel Base Single Crystals Across Length Scales*, Elsevier, 2022, pp. 107–139.

[46] E. A. Thornton, “Aerospace Thermal-Structural Testing Technology,” *Appl. Mech. Rev.*, vol. 50, no. 9, pp. 477–498, Sep. 1997, doi: 10.1115/1.3101738.

[47] Y. T. Tang *et al.*, “Alloys-by-design: Application to new superalloys for additive manufacturing,” *Acta Mater.*, vol. 202, pp. 417–436, 2021, doi: 10.1016/j.actamat.2020.09.023.

[48] B. Roebuck, J. Lord, and L. Orkney, “Validation of a Miniature Tensile Strength Measurement System,” in *Small Specimen Test Techniques: Fourth Volume*, 100 Barr Harbor Drive, PO Box C700, West Conshohocken, PA 19428-2959: ASTM International, pp. 234-234–17.

[49] A. Pignolet *et al.*, “Experimental Approach for Metals Mechanical Behavior Characterization at High Temperature: Development of a Complex Tensile Test Machine,” *Proceedings*, vol. 2, no. 8, p. 355, 2018, doi: 10.3390/icem18-05207.

[50] C. Kemper and G. Bringert, *Temperature measurements*. 2007.

[51] M. Trull and J. H. Beynon, “High temperature tension tests and oxide scale failure,” *Mater. Sci. Technol.*, vol. 19, no. 6, pp. 749–755, 2003, doi: 10.1179/026708303225003072.

[52] B. Song, K. Nelson, R. Lipinski, J. Bignell, and E. P. George, “Dynamic High-Temperature Tensile Characterization of an Iridium Alloy with Kolsky Tension Bar Techniques,” *J. Dyn. Behav. Mater.*, vol. 1, no. 3, pp. 290–298, 2015, doi: 10.1007/s40870-015-0022-6.

[53] A. Smalcerz and R. Przylucki, “Impact of electromagnetic field upon temperature measurement of induction heated charges,” *Int. J. Thermophys.*, vol. 34, no. 4, pp. 667–679, 2013, doi: 10.1007/s10765-013-1423-1.

[54] O. E. Inc., “What is a type K Thermocouple?,” 2022. https://www.omega.com/en-us/resources/k-type-thermocouples (accessed Feb. 9, 2023).

[55] H. Su, X. Fang, Z. Qu, C. Zhang, B. Yan, and X. Feng, “Synchronous Full-Field Measurement of Temperature and Deformation of C/SiC Composite Subjected to Flame Heating at High Temperature,” *Exp. Mech.*, vol. 56, no. 4, pp. 659–671, 2016, doi: 10.1007/s11340-015-0066-5.

[56] M. D. Novak and F. W. Zok, “High-temperature materials testing with full-field strain measurement: Experimental design and practice,” *Rev. Sci. Instrum.*, vol. 82, no. 11, 2011, doi: 10.1063/1.3657835.

[57] A. S. Morris and R. Langari, “Temperature Measurement,” in *Measurement and Instrumentation*, vol. 86, Elsevier, 2012, pp. 347–396.

[58] H. J. Jo, J. L. King, K. Blomstrand, and K. Sridharan, “Spectral emissivity of oxidized and roughened metal surfaces,” *Int. J. Heat Mass Transf.*, vol. 115, pp. 1065–1071, 2017, doi: 10.1016/j.ijheatmasstransfer.2017.08.103.

[59] G. Cao *et al.*, “In situ measurements of spectral emissivity of materials for very high temperature reactors,” *Nucl. Technol.*, vol. 175, no. 2, pp. 460–467, 2011, doi: 10.13182/NT11-A12317.

[60] D. L. Kelly, D. E. Scarborough, and B. S. Thurow, “A novel multi-band plenoptic pyrometer for high-temperature applications,” *Meas. Sci. Technol.*, vol. 32, no. 10, p. 105901, Oct. 2021, doi: 10.1088/1361-6501/ac0465.

[61] B. Pan, K. Qian, H. Xie, and A. Asundi, “Two-dimensional digital image correlation for in-plane displacement and strain measurement: a review,” *Meas. Sci. Technol.*, vol. 20, no. 6, p. 062001, Jun. 2009, doi: 10.1088/0957-0233/20/6/062001.

[62] Y. L. Dong and B. Pan, “A Review of Speckle Pattern Fabrication and Assessment for Digital Image Correlation,” *Exp. Mech.*, vol. 57, no. 8, pp. 1161–1181, 2017, doi: 10.1007/s11340-017-0283-1.

[63] W. S. LePage, J. A. Shaw, and S. H. Daly, “Optimum Paint Sequence for Speckle Patterns in Digital Image Correlation,” *Exp. Tech.*, vol. 41, no. 5, pp. 557–563, 2017, doi: 10.1007/s40799-017-0192-3.

[64] W. S. LePage, S. H. Daly, and J. A. Shaw, “Cross Polarization for Improved Digital Image Correlation,” *Exp. Mech.*, vol. 56, no. 6, pp. 969–985, 2016, doi: 10.1007/s11340-016-0129-2.

[65] T. Nozawa *et al.*, “Non-contact strain evaluation for miniature tensile specimens of neutron-irradiated F82H by digital image correlation,” *Fusion Eng. Des.*, vol. 157, no. April, p. 111663, 2020, doi: 10.1016/j.fusengdes.2020.111663.

[66] B. Pan, D. Wu, Z. Wang, and Y. Xia, “High-temperature digital image correlation method for full-field deformation measurement at 1200 °C,” *Meas. Sci. Technol.*, vol. 22, no. 1, 2011, doi: 10.1088/0957-0233/22/1/015701.

[67] Z. Pan, S. Huang, Y. Su, M. Qiao, and Q. Zhang, “Strain field measurements over 3000 °C using 3D-Digital image correlation,” *Opt. Lasers Eng.*, vol. 127, no. November 2019, p. 105942, 2020, doi: 10.1016/j.optlaseng.2019.105942.

[68] L. Yu, F. Ren, X. Zhang, and B. Pan, “Ultra-high temperature video extensometer: System development and experimental validation,” *Rev. Sci. Instrum.*, vol. 93, no. 4, 2022, doi: 10.1063/5.0085184.

[69] L. J. Rowley, T. Q. Thai, A. Dabb, B. D. Hill, B. A. Furman, and R. B. Berke, “High speed ultraviolet digital image correlation (UV-DIC) for dynamic strains at extreme temperatures,” *Rev. Sci. Instrum.*, vol. 93, no. 8, 2022, doi: 10.1063/5.0090534.

[70] L. Yu and B. Pan, “Overview of High-temperature Deformation Measurement Using Digital Image Correlation,” *Exp. Mech.*, vol. 61, no. 7, pp. 1121–1142, 2021, doi: 10.1007/s11340-021-00723-8.

[71] Y. Liu, L. Yu, Z. Wang, and B. Pan, “Neutralizing the impact of heat haze on digital image correlation measurements via deep learning,” *Opt. Lasers Eng.*, vol. 164, no. February, p. 107522, 2023, doi: 10.1016/j.optlaseng.2023.107522.

[72] M.-T. Lin, C. F. C. Sciammarella, L. Lamberti, P. L. Reu, M. A. Sutton, and C. H. Hwang, *Advancement of Optical Methods & Digital Image Correlation in Experimental Mechanics, Volume 3*, vol. 3. Cham: Springer International Publishing, 2019.

[73] P. Meyer and A. M. Waas, “Measurement of In Situ-Full-Field Strain Maps on Ceramic Matrix Composites at Elevated Temperature Using Digital Image Correlation,” *Exp. Mech.*, vol. 55, no. 5, pp. 795–802, 2015, doi: 10.1007/s11340-014-9979-7.

[74] J. Song, J. Yang, F. Liu, K. Lu, and Y. Yao, “Ultra-high temperature mechanical property test of C/C composites by a digital image correlation method based on an active laser illumination and background radiation suppressing method with multi-step filtering,” *Appl. Opt.*, vol. 58, no. 24, p. 6569, 2019, doi: 10.1364/ao.58.006569.

[75] S. Taylor, J. B. Wright, E. C. Forrest, B. Jared, J. Koepke, and J. Beaman, “Investigating relationship between surface topography and emissivity of metallic additively manufactured parts,” *Int. Commun. Heat Mass Transf.*, vol. 115, no. May, p. 104614, Jun. 2020, doi: 10.1016/j.icheatmasstransfer.2020.104614.

[76] M. W. Fu and W. L. Chan, “Geometry and grain size effects on the fracture behavior of sheet metal in micro-scale plastic deformation,” *Mater. Des.*, vol. 32, no. 10, pp. 4738–4746, 2011, doi: 10.1016/j.matdes.2011.06.039.

[77] D. L. Steinbrunner, D. K. Matlock, and G. Krauss, “Void formation during tensile testing of dual phase steels,” *Metall. Trans. A*, vol. 19, no. 3, pp. 579–589, 1988, doi: 10.1007/BF02649272.

[78] A. V. Sergueeva, J. Zhou, B. E. Meacham, and D. J. Branagan, “Gage length and sample size effect on measured properties during tensile testing,” *Mater. Sci. Eng. A*, vol. 526, no. 1–2, pp. 79–83, Nov. 2009, doi: 10.1016/j.msea.2009.07.046.

[79] W. G. Tilson and C. Katsarelis, “SLM Inconel 718 Thin Section Study -- Rev A,” Huntsville, AL, 2019.

[80] C. H. Yu *et al.*, “Thin-wall effects and anisotropic deformation mechanisms of an additively manufactured Ni-based superalloy,” *Addit. Manuf.*, vol. 36, no. June, p. 101672, 2020, doi: 10.1016/j.addma.2020.101672.

[81] B. L. Boyce *et al.*, “Extreme-Value Statistics Reveal Rare Failure-Critical Defects in Additive Manufacturing,” *Adv. Eng. Mater.*, vol. 19, no. 8, 2017, doi: 10.1002/adem.201700102.

[82] American Welding Society, AMSD20.1/D20.1M:2019: "Specification for Fabrication of Metal Components using Additive Manufacturing," 2019.

[83] NASA, NASA-STD-6030: “Additive Manufacturing Requirements for Spaceflight Systems,” 2021.

[84] C. Axial and F. Application, “Standard Guide for Additive Manufacturing — Test Artifacts — Accelerated Build Quality Assurance for Laser Beam Powder Bed Fusion,” pp. 1–5, doi: 10.1520/F3626-23.2.

[85] H. C. Taylor, E. A. Garibay, and R. B. Wicker, “Toward a common laser powder bed fusion qualification test artifact,” *Addit. Manuf.*, vol. 39, p. 101803, 2021, doi: 10.1016/j.addma.2020.101803.

[86] ASTM International, ISO/ASTM 52902-19: “Additive manufacturing — Test artefacts — Geometric capability assessment of additive Reference number,” 2019.

[87] M. A. de Pastre, S. C. Toguem Tagne, and N. Anwer, “Test artefacts for additive manufacturing: A design methodology review,” *CIRP J. Manuf. Sci. Technol.*, vol. 31, pp. 14–24, 2020, doi: 10.1016/j.cirpj.2020.09.008.

[88] M. Seifi *et al.*, “Progress Towards Metal Additive Manufacturing Standardization to Support Qualification and Certification,” *Jom*, vol. 69, no. 3, pp. 439–455, 2017, doi: 10.1007/s11837-017-2265-2.

[89] S. C. Jensen *et al.*, “Long-term process stability in additive manufacturing,” *Addit. Manuf.*, vol. 61, no. June 2022, p. 103284, 2023, doi: 10.1016/j.addma.2022.103284.

LIST OF SYMBOLS, ABBREVIATIONS, AND ACRONYMS

AFRL	Air Force Research Laboratory
AM	Additive Manufacturing
DIC	Digital Image Correlation
LVDT	Linear Variable Differential Transformer
ICME	Integrated Computational Materials Engineering
RVE	Representative Volume Element
RXNMB	Metals Behavior and Response Section, Composite, Ceramic, Metallic, and Materials Performance Division, Materials and Manufacturing Directorate
YS	Yield Strength
UTS	Ultimate Tensile Strength